Analytical investigation of the interfacial behavior of a prestressed concrete beam strengthened with a prestressed FRP-bonded plate

Hanane Mebsout[a], *Mohamed Atif* Benatta[b], *Baghdad* Krour[c], *Oussama* Benachour[d], *Mohamed* Bachir Bouiadjra[e], *Nacer* Rahal[f]

[a] Mustapha Stambouli University,
Mascara, People's Democratic Republic of Algeria,
e-mail: mebsouthanane@gmail.com,
ORCID iD: https://orcid.org/0009-0003-5837-4144

[b] University of Djillali Liabes, Structures and Advanced Materials in Civil Engineering and Public Works Laboratory (LSMAGCTP),
Sidi Bel Abbes, People's Democratic Republic of Algeria,
e-mail: bematif@gmail.com,
ORCID iD: https://orcid.org/0009-0007-5854-9054

[c] University of Djillali Liabes, Structures and Advanced Materials in Civil Engineering and Public Works Laboratory (LSMAGCTP),
Sidi Bel Abbes, People's Democratic Republic of Algeria,
e-mail: baghdad.krour@univ-sba.dz, **corresponding author**,
ORCID iD: https://orcid.org/0000-0002-8265-9807

[d] University of Djillali Liabes, Structures and Advanced Materials in Civil Engineering and Public Works Laboratory (LSMAGCTP),
Sidi Bel Abbes, People's Democratic Republic of Algeria,
e-mail: dr.oussama.benachour@gmail.com,
ORCID iD: https://orcid.org/0009-0003-3792-7424

[e] University of Djillali Liabes, Structures and Advanced Materials in Civil Engineering and Public Works Laboratory (LSMAGCTP),
Sidi Bel Abbes, People's Democratic Republic of Algeria +
Thematic Agency for Research in Science and Technology,
Algiers, People's Democratic Republic of Algeria,
e-mail: mohamedbachirbouiadjra@gmail.com,
ORCID iD: https://orcid.org/0009-0008-4814-6187

[f] Mustapha Stambouli University, Department of Civil Engineering,
Mascara, People's Democratic Republic of Algeria +
University of Sciences and Technology,
Laboratory of Mechanical Structure and Construction Stability, Oran, People's Democratic Republic of Algeria,
e-mail: n.rahal@univ-mascara.dz,
ORCID iD: https://orcid.org/0009-0002-0400-8360

https://doi.org/10.5937/vojtehg73-54215

ACKNOWLEDGMENT: The authors acknowledge the financial support received from the Algerian Ministry of Higher Education and Scientific Research. A grateful acknowledgement is also addressed to the Thematic Agency for Research in Science and Technology (ATRST) of Algeria.

FIELD: civil engineering, materials
ARTICLE TYPE: original scientific paper

Abstract:

Introduction/purpose: Utilizing composite materials to reinforce reinforced concrete structures is now a very prevalent practice in the field of civil engineering. However, prestressed concrete construction does not usually use this method. The principal purpose of the present study is to extend the use of composite materials to reinforce prestressed concrete beams by taking into account the effect of interfacial stresses concentration on the global behavior of such structures.

Methods: A new analytical model is suggested taking into account how changes in the RC beam's prestress affect the interface stresses. A polynomial function expressing the variation of the geometrical shape of the cable as well as the instantaneous and non-instantaneous losses of the prestressed concrete beam is considered in order to address the issue of stress concentration at the adhesive-plate-concrete interface.

Results: The main findings of the present investigation demonstrate that, in the presence of cable prestress, the interface stresses decrease non-significantly; but, as the prestressing force applied to the FRP plate increases, a more substantial increase of interfacial stresses is observed.

Conclusion: Because of a high degree of contact stresses at the plate end the debonding risk becomes greater and an anchoring mechanism is recommended at the edge of the plate.

Key words: prestressed concrete beam, FRP composites, interfacial stresses, fibers orientations, strengthening.

Introduction

The necessity for public works and civil engineering infrastructures to be improved has grown significantly in recent years, to the point that heritage preservation is one of the requirements that must be fulfilled to ensure ecologically responsible, sustainable growth. One of the ways to increase the safety and durability of these structures is reinforcement using several methods. Thus, many theoretical and experimental scientific studies have been carried out to recommend the best solutions for reinforcing existing reinforced concrete structures. One of these solutions is the use of composite material plates such as carbon fiber reinforced polymer (CFRP) plates due to their high stiffness and light weight.

A review paper on the use of prestressed composite materials in the strengthening of reinforced concrete beams was published by (Aslam et al, 2015) illustrating the benefits and drawbacks of several strengthening procedures, including external reinforcement (EBR), surface reinforcement (NSM), and externally post-tensioned techniques (EPT). Prestressed Near Surface Mounted Carbon Fiber Reinforced Polymer laminates (NSM-CFRP) were used in an experimental and numerical investigation by (Mostakhdemin Hosseini et al, 2016) to strengthen low resistance reinforced concrete slabs. The results indicate an intriguing improvement in the bearing capacity of slabs. The impact of a prestressed CFRP laminate on the fatigue performance of steel plates was investigated by (Emdad & Al-Mahaidi, 2015). It is shown in this experimental and numerical work that prestressed CFRP laminates dramatically reduce strain in steel plate specimens. A new experimental and numerical study on the bending behavior of reinforced concrete beams reinforced with prestressed CFRP laminates has been developed by Gao et al. (2016); this study's primary contribution is the application of a novel CFRP laminate prestressing method. An analytical method for a bending study of reinforced concrete beams reinforced by prestressed CFRP plates was proposed by (Rezazadeh et al, 2015). This method takes into account the maximum capacity of CFRP plate reinforced beams in cases when the first mode of delamination predominates. A moment-curvature connection is created based on three linear branches that correspond to the pre-cracking, post-cracking, and post-plastification stages. In a study given by (Bansal et al, 2016), the FRP laminates are swapped out for FRP sheets in an attempt to solve the issue of the debonding of laminates prior to fiber breakage.

A number of studies conducted by various experts indicate that the presence of shear and normal stresses at the plate–core interface is an important component. Researchers have devised numerous closed-form solutions for the interfacial stresses since they can, in fact, lead to brittle fracture of the concrete layer supporting the composite laminate and early collapse of the reinforced beam. The interfacial stresses are accurately estimated using Smith & Teng's solution (Smith & Teng, 2001); however, it ignores the fiber orientation of the FRP plate. To enhance the solution created by (Smith & Teng, 2001), further solutions have been put forth. (Tounsi et al, 2009) have suggested a novel method that ignores the orientation influence of fibers while also accounting for adherend shear deformations. A novel approach has been provided by (Tounsi & Benyoucef, 2007), which takes into account the fiber orientation of the FRP plate while keeping the flexural stiffness of composite plates in mind. A sensitivity analysis that takes into account various combinations of fiber orientations has been considered. An analytical analysis was conducted by (Krour et al, 2010, 2011) to provide a more precise solution for the interfacial stress problem by taking into account the mean curvature at the interface between the RC beam and the FRP plate and adjusting fiber spacing according to its thickness. Following that, an analytical and numerical investigation was carried out by (Krour et al, 2013) to determine the optimal approach for determining bearing capacity and interfacial stresses.

To achieve the time-dependent impact, numerous research studies were conducted. For example, Mohamed et al. (2009) carried out a theoretical interfacial stress analysis for simply supported RC beams with thin FRP composite plates, taking into account the laminate theory, the interface slip effect on the structural performance, and the same assumptions as (Smith & Teng, 2001). The analysis included both the creep and shrinkage effects. Similarly to this, (Fahsi et al, 2011) carried out an analytical analysis for interfacial adhesive stresses, including creep, shrinkage, and thermal deformation, using the mean curvature assumption between the two addends. Both investigations were carried out using the Fib-international model (1990).

Recently, prestressed laminates have been applied to bridge girders and other types of constructions in the field, with both theoretical and empirical investigations conducted. The analyses produced closed-form formulas that could be used to determine peeling stress and interfacial shear in beams that had laminates or bonded, non-prestressed plates. (Al-Emrani & Kliger, 2006) have addressed the issue of interfacial stress in the context of prestressed laminates used for strengthening and repair. The examined beam was not loaded throughout this experiment; only interfacial shear stress was examined. These investigations were all conducted on steel or reinforced concrete beams that were strengthened with CFRP plates, either prestressed or not. Using the laminate theory and altering the fiber orientation, (Benachour et al, 2008) conducted an analytical analysis of the interface steel beam reinforced by a prestressed CFRP plate.

Due to the significance of prestressed concrete, many studies have concentrated on the estimation of time-dependent losses. Indeed, (Páez & Sensale-Cozzano, 2021) proposed a theoretical analysis of simply supported and continuous unbonded prestressed concrete beams, taking into account concrete creep and shrinkage as well as pre-stressing steel relaxation. In order to ascertain the prestress loss and time-dependent deflection in cracked prestressed concrete elements, prestressed with fiber reinforced polymers or steel tendons, (Páez, 2023) carried out a novel, simplified method based on the creep-transformed section method. Artificial Intelligence has been applied to civil engineering challenges as a new contribution. Indeed, (Zhang et al, 2023) predicted the long-term prestress loss for prestressed concrete cylinder structures using machine learning. Using a numerical model calibrated against experimental data, (Lou & Karavasilis, 2018) gave an evaluation of the time-dependent behavior and the prediction of the long-term deflection of concrete beams prestressed with internal unbonded carbon fiber reinforced polymer (CFRP) tendons.

Because composite material plates are an effective way to reinforce steel or reinforced concrete structures, researchers are now concentrating their efforts on employing this technique to prestressed concrete, which is commonly used in civil engineering. An analytical study by (Mebsout et al, 2017) amply demonstrated the benefits of using prestressed FRP plates to enhance the behavior of prestressed concrete section beams. The study showed that it is possible to remove tensile stress by applying a prestressed CFRP plate transforming the cross-sectional area from Class II to Class I according to Eurocode 2 (Le Delliou, 2003).

This paper focuses on an analytical analysis of prestressed composite FRP plates used in conjunction with prestressed concrete beams for reinforcement. Based on the model developed by (Smith & Teng, 2001), the study consists of the analysis of normal and shear interfacial stresses for a prestressed concrete beam strengthened by a prestressed FRP composite plate, where (Smith & Teng, 2001) deal with RC beams reinforced with FRP plates. The beam is simply supported, and three load cases are considered. As a new contribution, the proposed model considers the immediate and time-dependent losses of the prestressed concrete beam in addition to the geometrical shape of the cable. This leads to a random fluctuation in the prestress losses along the span beam. However, this variation of the prestress can be approximated by a simple polynomial function necessary to facilitate the integration of the governing equations of interfacial stresses.

Interfacial shear and normal stresses governing equation

Previous research has shown that high stress concentration at the interface between the composite plate and concrete may compromise this type of reinforcement and cause the debonding of the composite plate. To estimate these contact stresses, an analytical model based on strain compatibility is developed in this section. Let us consider a simply supported prestressed beam represented in Figure 1 and Figure 2.

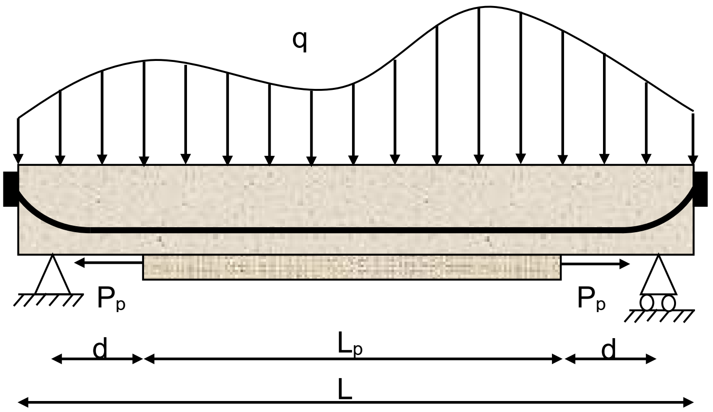

Figure 1 – Simply supported prestressed concrete beam strengthened with a bonded FRP plate

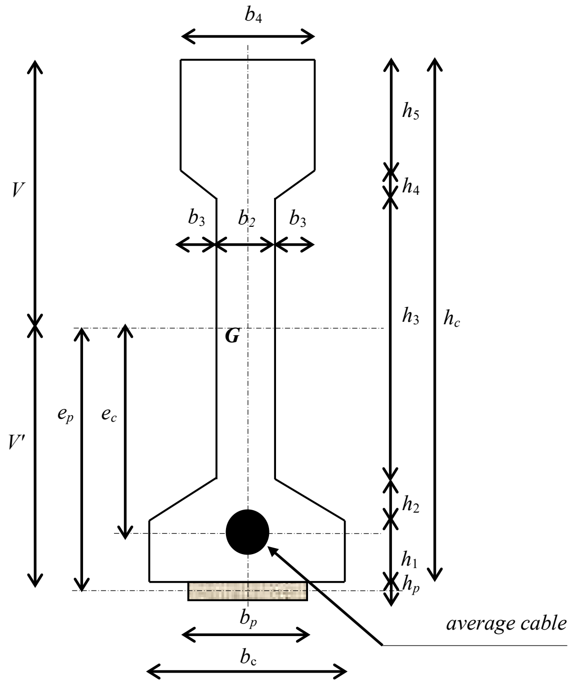

Figure 2 – Shape of the cross section

Figure 3 displays a differential segment, or dx, of the plated beam, with all forces and stresses indicated by their corresponding signs.

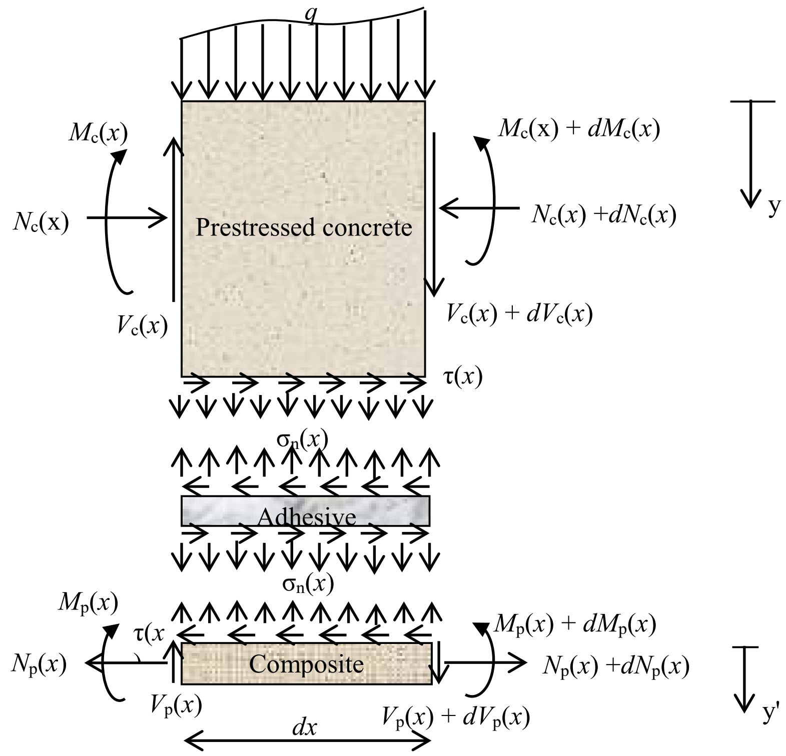

Figure 3 – Forces in the infinitesimal element of a soffit-plated beam

The interfacial shear and the normal stresses are represented by the symbols $\tau(x)$ and $\sigma(x)$, respectively.

The assumptions listed below are made:

1. The concrete, adhesive, and FRP materials behave elastically and linearly.
2. No slip is allowed at the interface of the bond (i.e., there is a perfect bond at the adhesive–concrete interface and at the adhesive–plate interface).
3. Stresses in the adhesive layer do not change with the thickness.
4. Deformations of adherends 1 and 2 are due to bending moments and axial forces.

5. Since the shear and normal stress equations can be uncoupled by assuming identical curvatures in the beam and the plate, the shear stress analysis makes this assumption due to a high stiffness of the concrete beam. Nevertheless, the peel stress solution does not make this assumption. Many authors, including (Smith & Teng, 2001), make advantage of this assumption.

The shear strain in the adhesive layer is expressed as:

$$\gamma_{xy} = \frac{\partial u(x,y)}{\partial y} + \frac{\partial w(x,y)}{\partial x} \approx \frac{u_p(x) - u_c(x)}{h_a}, \tag{1}$$

Consequently, the shear stress in the adhesive layer is given by:

$$\tau(x) = G_a \left[\frac{u_p(x) - u_c(x)}{h_a} \right], \tag{2}$$

where, G_a , t_a, u_p , and u_c indicate, in that order, the shear modulus, the thickness of the adhesive layer, the horizontal displacement at the top of the externally bonded FRP plate, and the horizontal displacement at the bottom of the concrete beam. The formula for shear stress in terms of the mechanical strain of the FRP plate $\varepsilon_p(x)$ and the concrete $\varepsilon_c(x)$ is obtained by differentiating Eq. (2) with regard to x.

$$\frac{d\tau(x)}{dx} = G_a \left[\frac{\varepsilon_p(x) - \varepsilon_c(x)}{h_a} \right], \tag{3}$$

The strain at the bottom of the prestressed concrete beam is given by:

$$\varepsilon_c(x) = \frac{du_c(x)}{dx} = \frac{y_c}{E_c I_c} M_c(x) - \frac{1}{E_c A_c} N_c(x), \tag{4}$$

where:

E_c is the elastic modulus, M_c is the bending moment, N_c is the axial force and y_c is the distance from the bottom of the concrete beam to its centroid.

The bending moment $M_c(x)$ results from the external loading and the prestress force applied with eccentricity from the centroid of the prestressed concrete beam. Then the bending moment $M_c(x)$ may be written as follows:

$$M_c(x) = M_q(x) + M_{pc}(x), \tag{5}$$

where:

$M_{pc}(x)$ is the bending moment due to the prestress force which can be written as follows:

$$M_{pc}(x) = P_c(x, \infty) \times e_c(x), \tag{6}$$

The present investigation employs the laminate theory (Herakovich, 1997) to underscore the impact of fiber orientation on the behavior of the externally bonded composite plate. Applying this theory to a symmetrical composite plate yields the following values for the composite plate curvature k_x and the mid-plane strain ε_x^0:

$$\begin{cases} \varepsilon_x^0 = A'_{11} N_x \dfrac{1}{b_2}, \\ k_x = D'_{11} M_x \dfrac{1}{b_2}, \end{cases} \tag{7}$$

where:

$[A'] = [A]^{-1}$ is the inverse of the extensional matrix $[A]$; $[D'] = [D]^{-1}$ is the inverse of the flexural matrix $[D]$; and b_2 is the width of the FRP plate.

The terms of the matrices $[A]$ and $[D]$ are written as:

$$\begin{cases} A_{mn} = \sum_{j=1}^{N} \overline{Q}_{mn} (h_j - h_{j-1}), \\ D_{mn} = \sum_{j=1}^{N} \overline{Q}_{mn} (h_j^3 - h_{j-1}^3), \end{cases} \tag{8}$$

where

$$\begin{cases} \overline{Q}_{11} = \left[\dfrac{E_{11}}{1-\nu_{12}\nu_{21}}\right]\cos^4(\theta_j) + \left[\dfrac{E_{22}}{1-\nu_{12}\nu_{21}}\right]\sin^4(\theta_j) \\ +2\left[\dfrac{\nu_{12}E_{22}}{1-\nu_{12}\nu_{21}} + 2G_{12}\right]\cos^2(\theta_j)\sin^2(\theta_j), \\ \overline{Q}_{22} = \left[\dfrac{E_{11}}{1-\nu_{12}\nu_{21}}\right]\sin^4(\theta_j) + \left[\dfrac{E_{22}}{1-\nu_{12}\nu_{21}}\right]\cos^4(\theta_j) \\ +2\left[\dfrac{\nu_{12}E_{22}}{1-\nu_{12}\nu_{21}} + 2G_{12}\right]\cos^2(\theta_j)\sin^2(\theta_j), \\ \overline{Q}_{12} = \dfrac{\nu_{12}E_{22}}{1-\nu_{12}\nu_{21}}\left[\cos^4(\theta_j) + \sin^4(\theta_j)\right] \\ +\left[\dfrac{E_{11}}{1-\nu_{12}\nu_{21}} + \dfrac{E_{22}}{1-\nu_{12}\nu_{21}} - 4G_{12}\right]\cos^2(\theta_j)\sin^2(\theta_j), \\ \overline{Q}_{33} = G_{12}, \end{cases} \tag{9}$$

where *j* is the number of the layer; *h;* $\left[\overline{Q}\right]$ and θ_j are respectively the thickness, the Hooke's elastic tensor and the fibers orientation of each layer.

Using the classical laminate theory (Herakovich, 1997), the strain at the top of CFRP plate is given by:

$$\varepsilon_p(x) = \frac{du_p(x)}{dx} = \varepsilon_x^0 - \frac{h_p}{2}k_x, \tag{10}$$

Substituting Eq. (7) in (10) gives the following equation:

$$\varepsilon_p(x) = A'_{11} \frac{N_p(x)}{b_p} - D'_{11} \frac{h_p}{2b_p} M_p(x), \tag{11}$$

The horizontal forces equilibrium gives:

$$\frac{dN_c(x)}{dx} = \frac{dN_p(x)}{dx} = b_p \tau(x), \tag{12}$$

And then:

$$N_c(x) = N_p(x) = b_p \int_0^x \tau(x) dx, \tag{13}$$

From the second assumption below (perfect bond), we obtain:

$$\frac{d^2 w_p(x)}{dx^2} = \frac{d^2 w_c(x)}{dx^2}, \tag{14}$$

The relationship between the moments in the two adherends can be written as follows:

$$M_c(x) = \Psi M_p(x), \tag{15}$$

with:

$$\Psi = -\frac{E_c I_c D'_{11}}{b_p}, \tag{16}$$

The moment equilibrium gives:

$$M_T(x) = M_c(x) + M_p(x) + N(x)\left[y_c + h_a + \frac{h_p}{2} \right], \tag{17}$$

where, $M_T(x)$ is the total applied moment.

In the case of the prestressed concrete beam, the bending moment is given by:

$$M_c(x) = M_q(x) + M_{Pc}(x) + M_{Pp}(x), \tag{18}$$

$$M_c(x) = M_q(x) + P_c(x,\infty)\times e_c(x) + P_p\left(y_c + h_a + \frac{h_p}{2}\right), \tag{19}$$

As a function of the total applied moment and the interfacial shear stress, the bending moments in each adherend are expressed as follows:

$$M_c(x) = -\frac{\Psi}{\Psi+1}\left[b_p\int_0^x \tau(x)(y_c + \frac{h_p}{2} + h_a)dx\right] + \frac{\Psi}{\Psi+1}M_T(x), \tag{20}$$

and

$$M_p(x) = -\frac{1}{\Psi+1}\left[b_p\int_0^x \tau(x)(y_c + \frac{h_p}{2} + h_a)dx\right] + \frac{1}{\Psi+1}M_T(x), \tag{21}$$

The first derivative of the bending moment in each adherend gives:

$$\frac{dM_c(x)}{dx} = \frac{\Psi}{\Psi+1}\left[V_T(x) - b_p\tau(x)(y_c + \frac{h_p}{2} + h_a)\right] \tag{22}$$

$$\frac{dM_p(x)}{dx} = \frac{1}{\Psi+1}\left[V_T(x) - b_p\tau(x)(y_c + \frac{h_p}{2} + h_a)\right], \tag{23}$$

Substituting Eqs. (4) and (11) into Eq. (3) and differentiating the resulting equation once yields:

$$\begin{aligned}\frac{d^2\tau(x)}{dx^2} &= \frac{G_a}{h_a}\left(\frac{A'_{11}}{b_p}\frac{dN_p(x)}{dx} - D'_{11}\frac{h_p}{2b_p}\frac{dM_p(x)}{dx}\right)\\ &+ \frac{G_a}{h_a}\left(\frac{1}{E_cA_c}\frac{dN_c(x)}{dx} - \frac{y_c}{E_cI_c}\frac{dM_c(x)}{dx}\right),\end{aligned} \tag{24}$$

Substituting Eqs. (22), (23) and Eq. (12) into Eq. (24) gives the following governing differential equation for the interfacial shear stress:

$$\frac{d^2\tau(x)}{dx^2}+\frac{G_a}{t_a}\left(\frac{\left(y_c+\frac{h_p}{2}\right)}{E_cI_cD'_{11}+b_p}D'_{11}\right)V_T(x)-\frac{G_a}{t_a}A'_{11}$$

$$-\frac{G_a}{t_a}\left(\frac{b_p}{E_cA_c}+\frac{\left(y_c+\frac{h_p}{2}\right)\left(y_c+h_a+\frac{h_p}{2}\right)}{E_cI_cD'_{11}+b_p}b_2D'_{11}\right)\tau(x)=0, \qquad (25)$$

$$V_T(x)=\frac{dM_T(x)}{dx}=\frac{dM_q(x)}{dx}+\frac{dM_{cp}(x)}{dx}+\frac{dM_{Pp}(x)}{dx}, \qquad (26)$$

Due to the losses of the prestressing force and the variable eccentricity of the mean cable along the beam span, the induced bending moment may be approximated by a polynomial function of the forth degree.

$$M_{cp}(x)=P_1x^4+P_2x^3+P_3x^2+P_4x+P_5, \qquad (27)$$

Then the shear effort induced by this moment is written as follows:

$$V_{cp}(x)=\frac{dM_{cp}(x)}{dx}=4P_1x^3+3P_2x^2+2P_3x+P_4, \qquad (28)$$

The coefficients P_i are determined by fitting the fluctuation of immediate and time-dependent losses and are specific to each case.

The general solutions presented below are limited to loading which is either concentrated or uniformly distributed, or both. For such loading $d^2V_q(x)/dx^2=0$, and the general solution to Eq. (26) is given by:

$$\tau(x)=C_1\cosh(\alpha x)+C_2\sinh(\alpha x)+\beta V_c(x)+\frac{\beta}{\alpha^2}\frac{d^2V_c(x)}{dx^2}, \qquad (29)$$

where:

$$\begin{cases} \alpha^2 = \dfrac{G_a}{h_a}\left(A'_{11} + \dfrac{b_p}{E_c A_c} + \dfrac{\left(y_c + \dfrac{h_p}{2}\right)\left(y_c + h_a + \dfrac{h_p}{2}\right)}{E_c I_c D'_{11} + b_p} b_p D'_{11} \right) \\ \beta = \dfrac{G_a}{h_a}\left(\dfrac{\left(y_c + \dfrac{h_p}{2}\right)}{E_c I_c D'_{11} + b_p} D'_{11} \right) \end{cases}, \tag{30}$$

$$\begin{cases} V_c(x) = V_q(x) + V_{cp}(x) + V_{P_0}(x) \\ \dfrac{d^2 V_c(x)}{dx^2} = \dfrac{d^2 V_{cp}(x)}{dx^2} = 24 P_1 x + 6 P_2 \end{cases}, \tag{31}$$

C_1 and C_2 are constant coefficients determined from the boundary conditions.

Adhesive normal stress: governing differential equations

The strain in the adhesive layer is given by:

$$\varepsilon_y = \frac{\partial w(x,y)}{\partial y} \approx \frac{w_p(x) - w_c(x)}{h_a}, \tag{32}$$

where $w_c(x)$ and $w_p(x)$ are the vertical displacements of the prestressed concrete beam and the CFRP plate, respectively.

The normal stress in the adhesive layer is expressed as follows:

$$\sigma_n(x) = \frac{E_a}{h_a}\left[w_p(x) - w_c(x) \right], \tag{33}$$

Differentiating Eq. (33) two times gives:

$$\frac{d^2\sigma_n(x)}{dx^2}=\frac{E_a}{h_a}\left[\frac{d^2w_p(x)}{dx^2}-\frac{d^2w_c(x)}{dx^2}\right], \tag{34}$$

The moment-curvature relationship for the two adherends is expressed as follows:

$$\begin{cases}\dfrac{d^2w_c(x)}{dx^2}=-\dfrac{M_c(x)}{E_cI_c}\\[2ex] \dfrac{d^2w_p(x)}{dx^2}=-\dfrac{D'_{11}M_p(x)}{b_p}\end{cases}, \tag{35}$$

The moment equilibrium of the prestressed concrete beam and the CFRP plate gives:

The prestressed concrete beam:

$$\begin{cases}\dfrac{dM_c(x)}{dx}=V_c(x)-b_py_c\tau(x)\\[2ex] \dfrac{dV_c(x)}{dx}=-b_p\sigma_n(x)-q\end{cases}, \tag{36}$$

The CFRP plate:

$$\begin{cases}\dfrac{dM_p(x)}{dx}=V_p(x)-b_p\dfrac{t_p}{2}\tau(x)\\[2ex] \dfrac{dV_p(x)}{dx}=b_p\sigma_n(x)\end{cases}, \tag{37}$$

Using the above equilibrium equations, the governing differential equations for the deflection of each adherend are given by:

The prestressed concrete beam:

$$\frac{d^4w_c(x)}{dx^4}=\frac{1}{E_cI_c}b_p\sigma_n(x)+\frac{y_c}{E_cI_c}b_p\frac{d\tau(x)}{dx}+\frac{q}{E_cI_c}, \tag{38}$$

The CFRP plate:

$$\frac{d^4 w_p(x)}{dx^4} = -D'_{11}\sigma_n(x) + D'_{11}\frac{h_p}{2}\frac{d\tau(x)}{dx}, \tag{39}$$

Substituting both Eqs. (38) and (23) as well as Eq. (39) into the fourth derivation of the interfacial normal stress obtained from Eq. (33) gives the following governing differential equation for the interfacial normal stress:

$$\begin{aligned}&\frac{d^4\sigma_n(x)}{dx^4} + \frac{E_a}{h_a}\left(D'_{11} + \frac{b_p}{E_c I_c}\right)\sigma_n(x)\\ &-\frac{E_a}{h_a}\left(D'_{11}\frac{h_p}{2} - \frac{y_c b_p}{E_c I_c}\right)\frac{d\tau(x)}{dx} + \frac{qE_a}{E_c I_c} = 0,\end{aligned} \tag{40}$$

The general solution of Eq. (40) which is a fourth-order differential equation is:

$$\begin{aligned}&\sigma(x) = e^{-\gamma x}\left[C_3\cos(\gamma x) + C_4\sin(\gamma x)\right] + e^{\gamma x}\left[C_5\cos(\gamma x) + C_6\sin(\gamma x)\right]\\ &-\eta_1\frac{d\tau(x)}{dx} - \eta_2 q,\end{aligned} \tag{41}$$

For large values of x, the normal interfacial stress is assumed to be zero, and so $C_5 = C_6 = 0$.

The general equation becomes:

$$\sigma_n(x) = e^{-\gamma x}\left[C_3\cos(\gamma x) + C_4\sin(\gamma x)\right] - \eta_1\frac{d\tau(x)}{dx} - \eta_2 q, \tag{42}$$

where:

$$
\begin{cases}
\gamma = \sqrt[4]{\dfrac{E_a}{4h_a}\left(D'_{11} + \dfrac{b_p}{E_c I_c}\right)} \\
\eta_1 = \dfrac{y_c b_p - E_c I_c D'_{11}\left(\dfrac{h_p}{2}\right)}{E_c I_c D'_{11} + b_p} \\
\eta_2 = \dfrac{1}{E_c I_c D'_{11} + b_p}
\end{cases}, \tag{43}
$$

The constant coefficients C_3 and C_4 are determined by the boundary conditions.

Application of the boundary conditions and closed-form solutions

The following boundary conditions are thus considered:

$$
\begin{cases}
N_c(0) = P(d,t) \\
N_p(0) = P_p \\
M_p(0) = 0 \\
\tau\left(L_p / 2\right) = 0
\end{cases}, \tag{44}
$$

These boundary conditions give the interfacial shear stress described by (Smith & Teng, 2001) and written as:

Uniformly distributed load

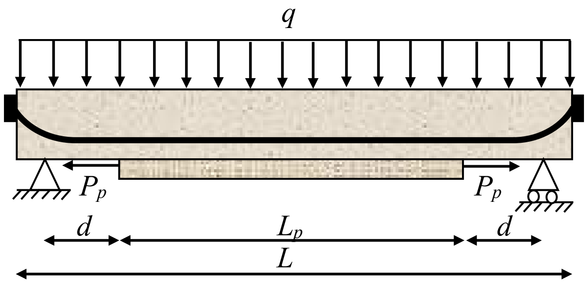

Figure 9 – Uniformly distributed load

$$\begin{cases} C_2 = \dfrac{G_a}{\alpha t_a}\left(\dfrac{A'_{11}}{b_p}P_p + \dfrac{1}{E_c A_c}P(d) - \dfrac{y_c}{E_c I_c}M_c(d)\right) - \dfrac{\beta}{\alpha}\dfrac{dV_c(d)}{dx} - \dfrac{\beta}{\alpha^3}\dfrac{d^3V_c(d)}{dx^2} \\ M_c(d) = \left(L-d\right)\dfrac{qd}{2} + P_p\left((y_c + h_a + \dfrac{h_p}{2}\right) + P_1 d^4 + P_2 d^3 + P_3 d^2 + P_4 d + P_5 \\ \dfrac{dV_c(d)}{dx} = \dfrac{dV_{cp}(d)}{dx^2} = 12P_1 d^2 + 6P_2 d + 2P_3 \\ \dfrac{d^3V_c(d)}{dx^2} = \dfrac{d^3V_{cp}(d)}{dx^2} = 24P_1 \\ C_1 = -C_2 \end{cases}, \quad (45)$$

Single point load

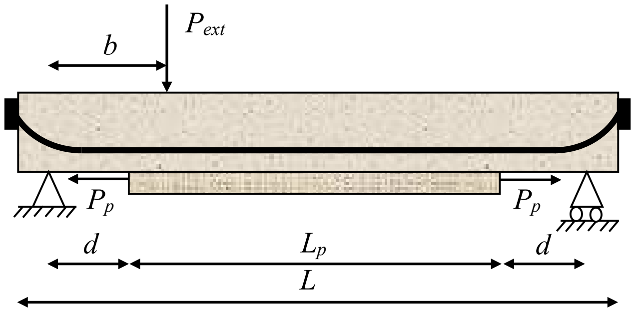

Figure 10 – Single point load

For such a loading type, two cases are possible: the first considers that the left edge of the plate is located to the left of the load application point $d < b$, and the second considers that the left edge of the plate is placed to the right of the load application point $d > b$.

Based on the general solution of Equation (45), applying the same boundary conditions as for the uniformly distributed load, and taking into account the continuity of the interface tangential stress and its first derivative at the application load point, we obtain:

For $d < b$:

$$\begin{cases} C_2 = \dfrac{G_a}{\alpha t_a}\left(\dfrac{A'_{11}}{b_p}P_p + \dfrac{1}{E_c A_c}P(d) - \dfrac{y_c}{E_c I_c}M_c(d)\right) - \dfrac{\beta}{\alpha}\dfrac{dV_c(d)}{dx} - \dfrac{\beta}{\alpha^3}\dfrac{d^3 V_c(d)}{dx^2} \\ M_c(d) = P_{ext}d\left(1-\dfrac{b}{L}\right) + P_1 d^4 + P_2 d^3 + P_3 d^2 + P_4 d + P_5 \\ \dfrac{dV_c(d)}{dx} = \dfrac{dV_{cp}(d)}{dx^2} = 12P_1 d^2 + 6P_2 d + 2P_3 \\ \dfrac{d^3 V_c(d)}{dx^2} = \dfrac{d^3 V_{cp}(d)}{dx^2} = 24P_1 \\ C_1 = -C_2 \end{cases} \quad , \tag{46}$$

For $d > b$:

$$\begin{cases} C_2 = \dfrac{G_a}{\alpha t_a}\left(\dfrac{A'_{11}}{b_p}P_p + \dfrac{1}{E_c A_c}P(d) - \dfrac{y_c}{E_c I_c}M_c(d)\right) - \dfrac{\beta}{\alpha}\dfrac{dV_c(d)}{dx} - \dfrac{\beta}{\alpha^3}\dfrac{d^3 V_c(d)}{dx^2} \\ M_c(d) = P_{ext}d\left(1-\dfrac{b}{L}\right) + P_p\left((y_c + h_a + \dfrac{h_p}{2}\right) \\ +P_1 d^4 + P_2 d^3 + P_3 d^2 + P_4 d + P_5 \\ \dfrac{dV_c(d)}{dx} = \dfrac{dV_{cp}(d)}{dx^2} = 12P_1 d^2 + 6P_2 d + 2P_3 \\ \dfrac{d^3 V_c(d)}{dx^2} = \dfrac{d^3 V_{cp}(d)}{dx^2} = 24P_1 \\ C_1 = -C_2 \end{cases} \quad , \tag{47}$$

Two symmetrical point loads

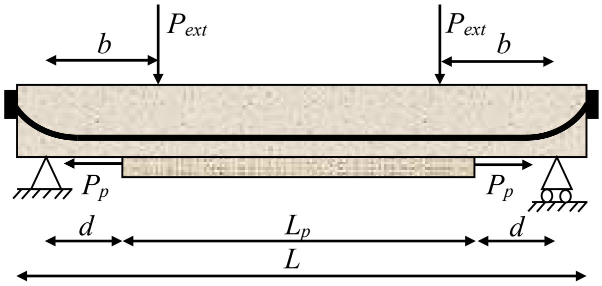

Figure 11 – Two symmetrical point loads

In the same way as for a single concentrated load, it is possible to obtain the expression of the tangential interface stress for two concentrated loads, taking into account the symmetry. The expression of the tangential stress is given by:

$d < b:$

$$\begin{cases} C_2 = \dfrac{G_a}{\alpha t_a}\left(\dfrac{A'_{11}}{b_p} P_p + \dfrac{1}{E_c A_c} P(d) - \dfrac{y_c}{E_c I_c} M_c(d)\right) - \dfrac{\beta}{\alpha}\dfrac{dV_c(d)}{dx} - \dfrac{\beta}{\alpha^3}\dfrac{d^3 V_c(d)}{dx^2} \\ M_c(d) = P_{ext} d + P_1 d^4 + P_2 d^3 + P_3 d^2 + P_4 d + P_5 \\ \dfrac{dV_c(d)}{dx} = \dfrac{dV_{cp}(d)}{dx^2} = 12 P_1 d^2 + 6 P_2 d + 2 P_3 \\ \dfrac{d^3 V_c(d)}{dx^2} = \dfrac{d^3 V_{cp}(d)}{dx^2} = 24 P_1 \\ C_1 = -C_2 \end{cases}, \quad (48)$$

$d > b:$

$$\begin{cases} C_2 = \dfrac{G_a}{\alpha t_a}\left(\dfrac{A'_{11}}{b_p}P_p + \dfrac{1}{E_c A_c}P(d) - \dfrac{y_c}{E_c I_c}M_c(d)\right) - \dfrac{\beta}{\alpha}\dfrac{dV_c(d)}{dx} - \dfrac{\beta}{\alpha^3}\dfrac{d^3 V_c(d)}{dx^2} \\ M_c(d) = P_{ext}d + P_p\left((y_c + h_a + \dfrac{h_p}{2}\right) \\ +P_1 d^4 + P_2 d^3 + P_3 d^2 + P_4 d + P_5 \\ \dfrac{dV_c(d)}{dx} = \dfrac{dV_{cp}(d)}{dx^2} = 12P_1 d^2 + 6P_2 d + 2P_3 \\ \dfrac{d^3 V_c(d)}{dx^2} = \dfrac{d^3 V_{cp}(d)}{dx^2} = 24P_1 \\ C_1 = -C_2 \end{cases} \quad , \qquad (49)$$

The constant coefficients C_3 and C_4 for the normal interfacial stress are given by:

$$\begin{cases} C_3 = \dfrac{E_a}{2\gamma^3 t_a E_c I_c}\left[V_T(0) + \gamma M_T(0)\right] - \dfrac{\eta_3}{2\gamma^3}\tau(0) + \dfrac{\eta_1}{2\gamma^3}\left(\dfrac{d^4\tau(0)}{dx^4} + \gamma\dfrac{d^3\tau(0)}{dx^3}\right) \\ C_4 = \dfrac{E_a}{2\gamma^2 t_a E_c I_c}M_T(0) - \dfrac{\eta_1}{2\gamma^2}\dfrac{d^3\tau(0)}{dx^3} \\ \eta_3 = \dfrac{E_a b_2}{t_a}\left(\dfrac{y_c}{E_c A_c} - \dfrac{D'_{11}t_2}{2b_2}\right) \end{cases} \quad , \qquad (50)$$

The aforementioned constant expressions C_3 and C_4 have been left in terms of the bending moment $M_T(0)$ and the shear force $V_T(0)$ at the end of the soffit plate. With the constants C_3 and C_4 calculated, Eq. (42) may be used to calculate the adhesive normal stress for all three load scenarios.

Results and discussions

As part of the present work on strengthening existing prestressed concrete beams using composite materials, a demonstration study on a prestressed bridge girder is conducted to examine potential practical problems that could occur from applying strengthening technologies to already-existing structures. The main goal is to demonstrate the existence of a high level of interfacial stresses leading to early debonding failure of laminates especially at their ends.

Additionally, it was noted that there is a knowledge gap regarding the best way to choose the adhesives and material properties for prestressed composite materials to minimize the amount of shear and normal stresses at the laminate ends without compromising the effectiveness of the strengthening technique.

For these reasons, a real case is examined. A simply supported bridge girder having a free span of 26 meters, is considered. The data used in this study are summarized in Table 1 and Figure 12. The laminate is kept at a constant width of 200 mm and a constant length of 24.6 m, with 0.7 m remaining between the end of the laminate and each support. The maximum shear and normal stress values in the bonding region depend on a number of factors. The prestressing force and the fiber orientation in various laminate layers are two most crucial factors for retrofitting beams.

Table 1 – Geometric characteristics of the cross section

h_c (mm)	h_1 (mm)	h_2 (mm)	h_3(mm)	h_4(mm)	h_5 (mm)	h_p (mm)	e_c (mm)
1300	270	150	700	100	80	1.2	476
b_c(mm)	b_2 (mm)	b_3 (mm)	b_4 (mm)	b_p (mm)	V (mm)	V' (mm)	e_p (mm)
500	150	100	350	200	674	626	627.1

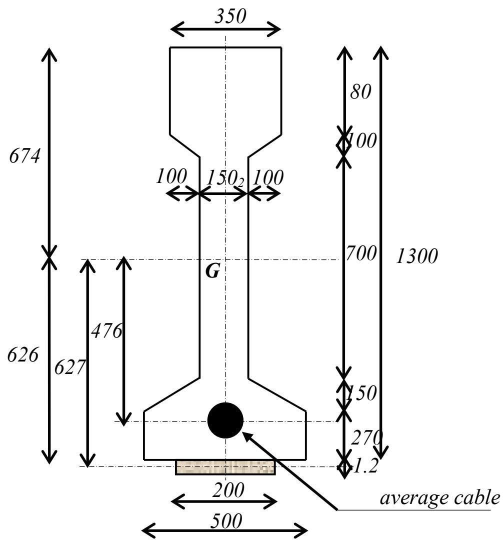

Figure 12 – Cross section sketch

Adhesive stresses with respect to the prestressing force P_p

Three example problems are taken into consideration. The first problem involves a beam that is simply supported and subjected to a uniformly distributed load (UDL), while the second problem involves a single point load and the third problem involves two symmetric point loads.

The UDL is taken to be equal to 100kN/m, the single point load is 500kN and the two symmetric point loads are P_{ext}=250kN and P_{ext}=250kN. Four values of P_p are considered in this study (0, 50, 100 and 150kN). For all the three problems, a unidirectional composite plate is used and the instantaneous elastic modulus of concrete is considered.

By way of comparison, we considered the work of (Benachour et al, 2008), which deals with the problem of interface stresses for a reinforced concrete beam. This will allow us to distinguish the effect of a prestressing cable on interface stresses.

Shear and normal interfacial stresses for UDL

The variation of normal stress and interfacial shear for the prestressed concrete beam reinforced with a bonded prestressed FRP plate along its span for the UDL scenario is shown in Figs. 13 and 14. The numerical values at the plate end are summarized in Table 2.

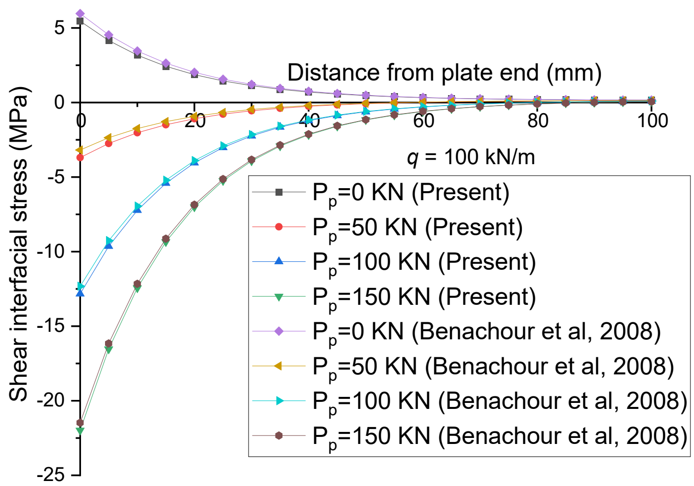

Figure 13 – Adhesive shear stress at the bond line for the FRP-strengthened beam under various prestressing forces Pp (the beam is under UDL)

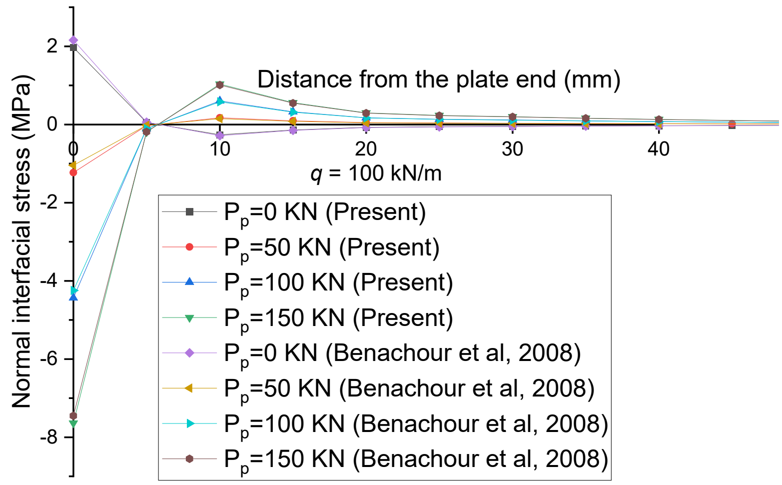

Figure 14 – Adhesive normal stress at the bond line for the FRP-strengthened beam under various prestressing forces Pp (the beam is under UDL)

Table 2 – Shear and normal interfacial stress at the plate end under UDL

Pp (KN)	$\tau(0)$ (Mpa)		$\sigma(0)$ (Mpa)	
	Concrete beam	*Prestressed concrete beam*	*Concrete beam*	*Prestressed concrete beam*
0	*5.965*	*5.456*	*2.158*	*1.971*
50	*-3.180*	*-3.689*	*-1.044*	*-1.231*
100	*-12.326*	*-12.835*	*-4.247*	*-4.435*
150	*-21.472*	*-21.981*	*-7.450*	*-7.638*

Shear and normal interfacial stresses for a single point load

The fluctuation of normal stress and interfacial shear for the prestressed concrete beam reinforced with a bonded prestressed FRP plate along its span for a single point load is depicted in Figs. 15 and 16. The edge values are reported in Table 5.

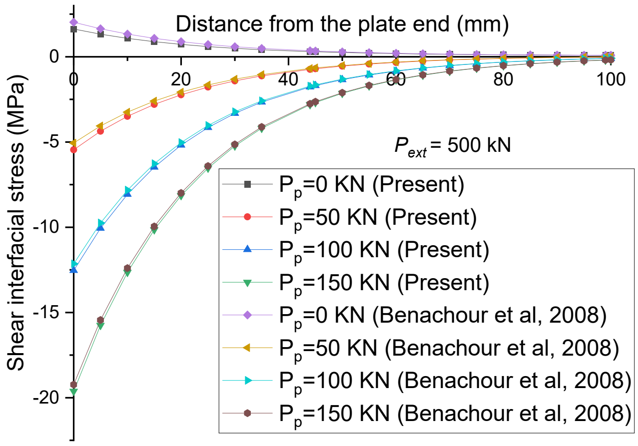

Figure 15 – Adhesive shear stress at the bond line for the FRP-strengthened beam under various prestressing forces Pp (the beam is under a single point load)

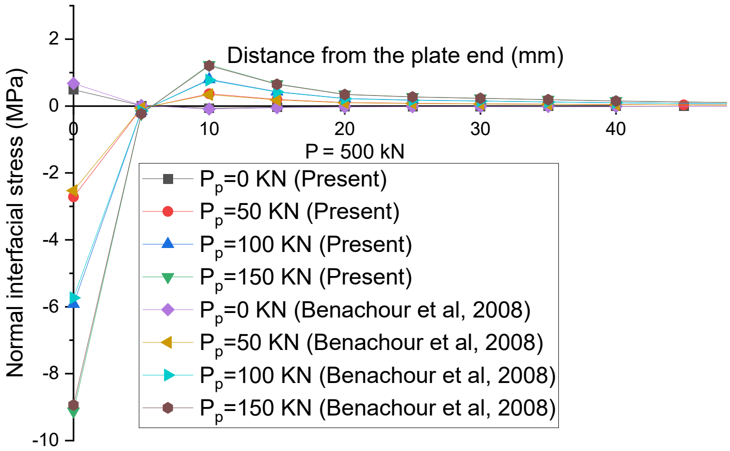

Figure 16 – Adhesive normal stress at the bond line for the FRP-strengthened beam under various prestressing forces Pp (the beam is under a single point load)

Table 3 – Shear and normal interfacial stress at the plate end under a single point load

Pp (KN)	$\tau(0)$ (Mpa)		$\sigma(0)$ (Mpa)	
	Concrete beam	Prestressed concrete beam	Concrete beam	Prestressed concrete beam
0	2.024	1.630	0.674	0.486
50	-5.059	-5.453	-2.528	-2.716
100	-12.143	-12.538	-5.732	-5.919
150	-12.143	-19.622	-8.935	-9.122

VOJNOTEHNIČKI GLASNIK / MILITARY TECHNICAL COURIER, 2025, Vol. 73, Issue 2

Shear and normal interfacial stresses for a two symmetric point load

The prestressed concrete beam reinforced with a bonded prestressed FRP plate exhibits variations in interfacial shear and normal stress along its span for a two point load, as shown in Figs. 17 and 18. The effect of the presstressing effort on the maximum interfacial stresses is shown in Table 6.

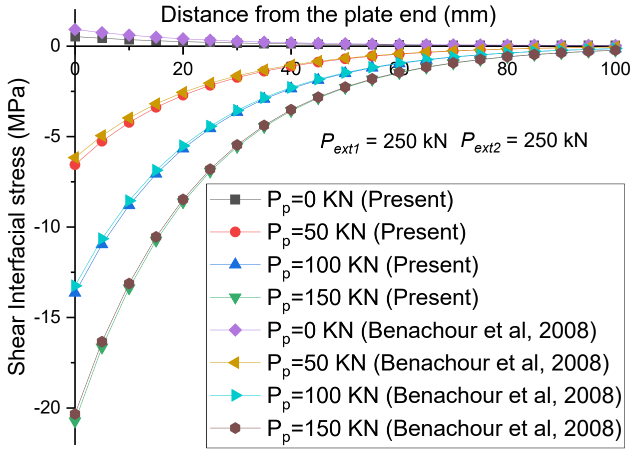

Figure 17 – Adhesive shear stress at the bond line for the FRP-strengthened beam under various prestressing forces Pp (the beam is under two symmetric point loads)

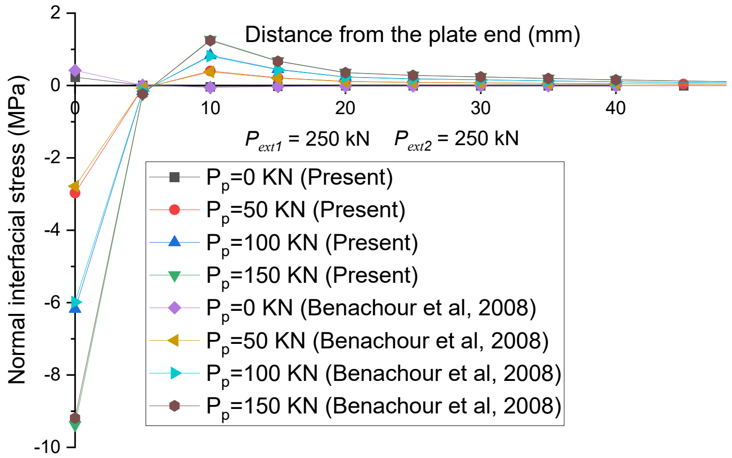

Figure 18 – Adhesive normal stress at the bond line for the FRP-strengthened beam under various prestressing forces Pp (the beam is under two symmetric point loads)

Table 4 – Shear and normal interfacial stress at the plate end under two symmetric point loads

Pp (KN)	$\tau(0)$ (Mpa)		$\sigma(0)$ (Mpa)	
	Concrete beam	Prestressed concrete beam	Concrete beam	Prestressed concrete beam
0	0.920	0.526	0.418	0.231
50	-6.164	-6.558	-2.784	-2.971
100	-13.248	-13.642	-5.987	-6.175
150	-20.332	-20.727	-9.190	-9.378

As it can be seen from the preceding figures, most interfacial stresses happen at the ends of adhesively attached plates and they start to decrease about 20 mm from the ends. Significant stress concentrations are also observed in the vicinity of the plate end when the prestressing force P_p value is increased. In contrast to a reinforced concrete beam, a small reduction in interfacial stresses is noted for the beams prestressed by a cable.

Effect of fiber orientation

Figures 19–24 illustrate how various fiber orientations affect adhesion stresses when viewed from the longitudinal direction of a beam. A 150 KN prestressing force is taken into account in the theoretical parametric analysis.

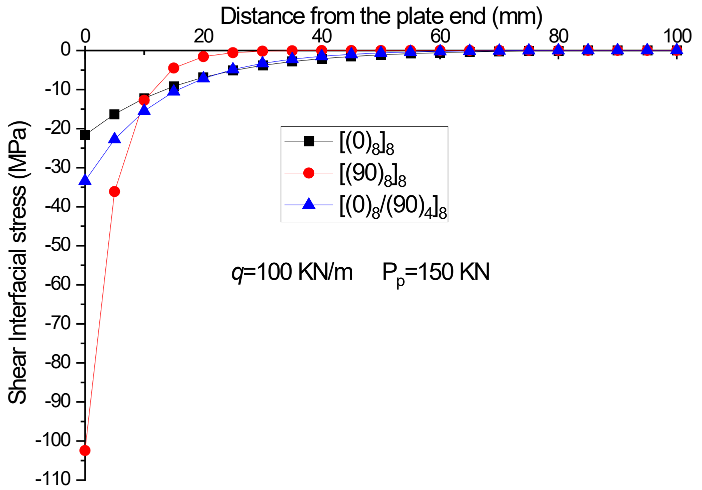

Figure 19 – Interfacial shear stress for a prestressed concrete beam with a bonded prestressed CFRP soffit plate having different fiber orientations (the beam is under UDL)

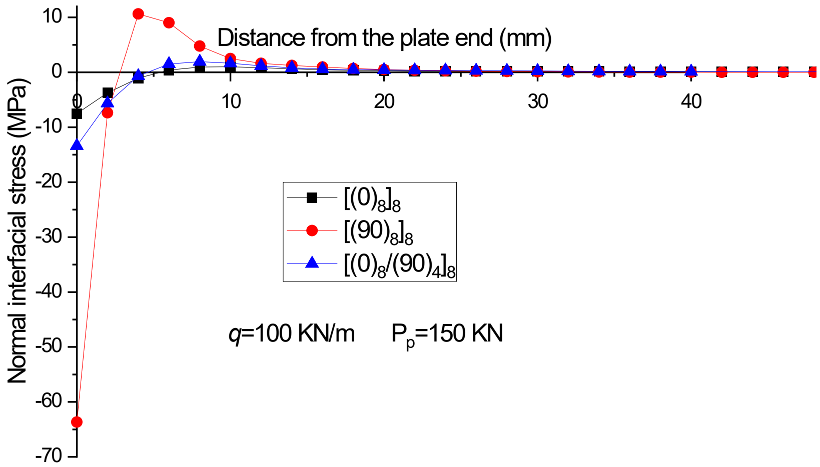

Figure 20 – Interfacial normal stress for a prestressed concrete beam with a bonded prestressed CFRP soffit plate having different fiber orientations (the beam is under UDL)

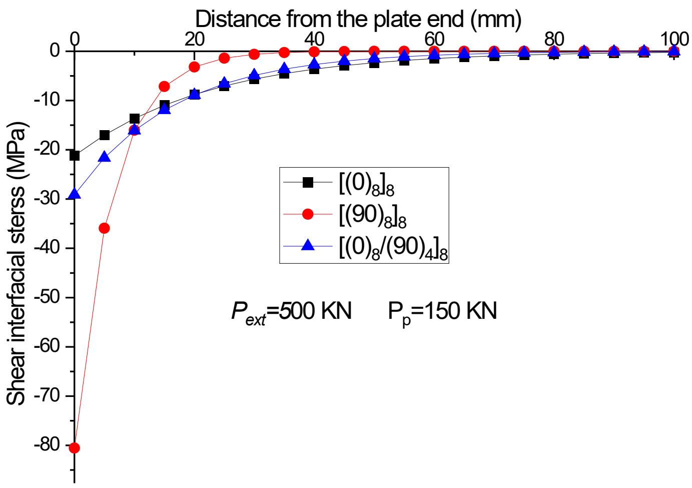

Figure 21 – Interfacial shear stress for a prestressed concrete beam with a bonded prestressed CFRP soffit plate having different fiber orientations (the beam is under a single point load)

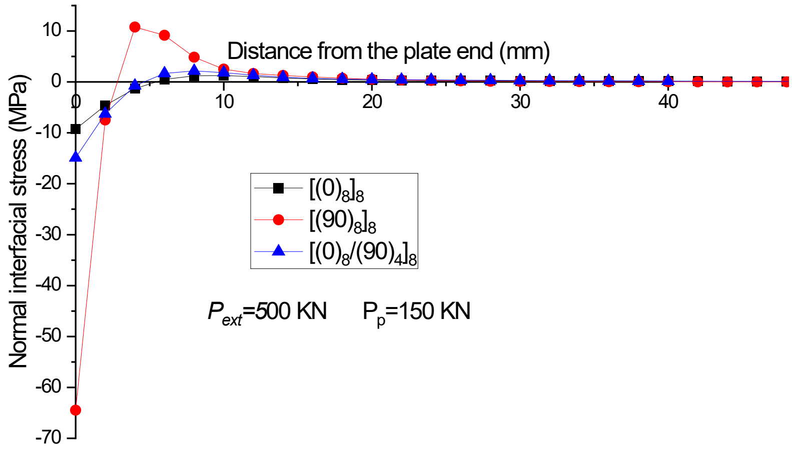

Figure 22 – Interfacial normal stress for a prestressed concrete beam with a bonded prestressed CFRP soffit plate having different fiber orientations (the beam is under a single point load)

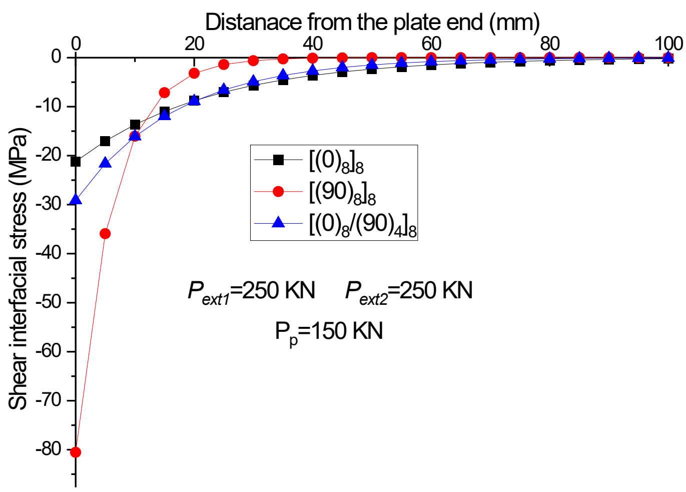

Figure 23 – Interfacial shear stress for a prestressed concrete beam with a bonded prestressed CFRP soffit plate having different fiber orientations (the beam is under two symmetric point loads)

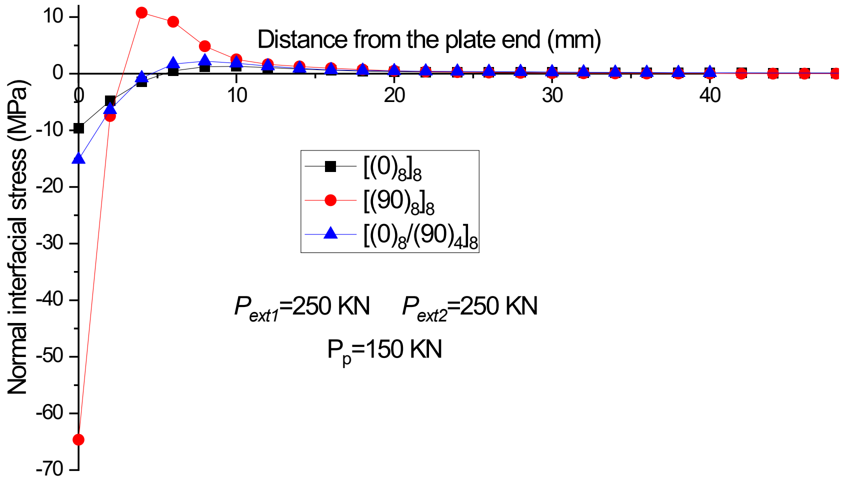

Figure 24 – Interfacial normal stress for a prestressed concrete beam with a bonded prestressed CFRP soffit plate having different fiber orientations (the beam is under two symmetric point loads)

The effective modulus of the composite plate varies when a fiber-reinforced polymer plate with various orientations is used. Fibers oriented towards the direction of the beam would increase the plate modulus, while fibers oriented perpendicular to the direction of the beam would significantly decrease the plate modulus. The effects of various fiber orientations on adhesion stresses as measured from the longitudinal direction of the beam are displayed in Figs. 10–15.

The FRP plate with fibers aligned perpendicular to the beam axis has the highest interfacial stresses, as shown in the above figures. This is in contrast to the findings of (Krour et al, 2013) who showed by a numerical study that the CFRP plate with fibers aligned perpendicular to the beam axis has the lowest interfacial stresses. It is also important to note that, with a prestressed CFRP plate, Bencahour et al. (2008) and Benali et al. (2023) arrived at the same conclusion as the current investigation.

Conclusion

This paper proposes a new analytical model to determine interfacial stresses for prestressed concrete beams reinforced by prestressed fiber-reinforced polymer (FRP) plates.

The model used takes into account the geometric shape of the cable along the span beam evolution as well as immediate and time-dependent losses expressed in terms of a polynomial function.

The model reveals the following main findings:

- A slight decrease in interfacial stresses is observed for prestressed concrete beams.
- Prestressing the FRP plate significantly raises the interfacial stresses, especially at the open edges of the plate.
- Prestressing the composite plate eliminates the effect of fiber orientation and maintains the lowest level of interface stress for fiber orientation in the longitudinal direction of the beam, enabling efficient use of the composite in the sense of its greater stiffness.
- The height level of interfacial stresses eventually results in the adoption of an anchoring mechanism that makes it possible to fix properly the composite plate.

In light of this, the investigation can be expanded to look at how time affects the general behavior of older prestressed buildings. Both the interface behavior and the cross-sectional behavior can be investigated in further detail.

References

Al-Emrani, M. & Kliger, R. 2006. Analysis of interfacial shear stresses in beams strengthened with bonded prestressed laminates. *Composites. Part B: Engineering*, 37(4-5), pp.265-272. Available at: https://doi.org/10.1016/j.compositesb.2006.01.004.

Aslam, M., Shafigh, P., Jumaat, M.Z. & Shah, S.N.R. 2015. Strengthening of RC beams using prestressed fiber reinforced polymers – A review. *Construction and Building Materials*, *82*, pp.235-256. Available at: https://doi.org/10.1016/j.conbuildmat.2015.02.051.

Bansal, P.P., Sharma, R. & Mehta, A. 2016. Retrofitting of RC girders using pre-stressed CFRP sheets. *Steel and Composite Structures*, 20(4), pp.833-849. Available at: https://doi.org/10.12989/scs.2016.20.4.833.

Benachour, A., Benyoucef, S., Tounsi, A. & Adda bedia, E.A. 2008. Interfacial stress analysis of steel beams reinforced with bonded prestressed FRP plate. *Engineering Structures*, 30(11), pp.3305-3315. Available at: https://doi.org/10.1016/j.engstruct.2008.05.007.

Benali, K., Krour, B., Atif Benatta, M., Hafid, K., Bachir Bouiadjra, M., Mechab, I. & Bernard, F. 2023. Investigation of dynamic behavior of prestressed FRP plate intended for strengthening prestressed RC beam. *Engineering structures*, 280, art.number:115690. Available at: https://doi.org/10.1016/j.engstruct.2023.115690.

Emdad, M.R. & Al-Mahaidi, R. 2015. Effect of prestressed CFRP patches on crack growth of centre-notched steel plates. *Composite Structures*, 123, pp.109-122. Available at: https://doi.org/10.1016/j.compstruct.2014.12.007.

Fahsi, B., Benrahou, K.-H., Krour, B., Tounsi, A., Benyoucef, S. & Bedia, E.A.A. 2011. Analytical analysis of interfacial stresses in FRP-RC hybrid beams with time-dependent deformations of RC beam. *Acta Mechanica Solida Sinica*, 24(6), pp.519-526. Available at: https://doi.org/10.1016/s0894-9166(11)60052-9.

-Fib-international. 1990. CEB-FIP Model Code 1990 - 1st Draft - Vol. 1, chapters 1-5. *FIB - International Federation for Structural Concrete* [online]. Available at: https://www.fib-international.org/publications/ceb-bulletins/ceb-fip-model-code-1990,-first-draft-vol-1-pdf-detail.html [Accessed: 15 October 2024].

Herakovich, C.T. 1997. *Mechanics of Fibrous Composites*. Wiley. ISBN: 978-0-471-10636-4.

Krour, B., Bernard, F. & Tounsi, A. 2013. Fibers orientation optimization for concrete beam strengthened with a CFRP bonded plate: A coupled analytical–numerical investigation. *Engineering Structures*, 56, pp.218-227. Available at: https://doi.org/10.1016/j.engstruct.2013.05.008.

Krour, B., Tounsi, A., Benyoucef, S. & Adda Bedia, E.A. 2010. An improved closed-form solution to interfacial stresses in rc beams strengthened with a composite plate. *Mechanics of Composite Materials*, 46(3), pp.331-340. Available at : https://doi.org/10.1007/s11029-010-9150-1.

Krour, B., Tounsi, A. & Meftah, S.A. 2011. A New Approach for Adhesive Stress Analysis of a Beam Bonded with Composite Plate Having Variable Fiber Spacing. *Composite Interfaces*, 18(2), pp.135-149. Available at https://doi.org/10.1163/092764411x567413.

Le Delliou, P. 2003. *Béton précontraint aux Eurocodes*. Presses Universitaires Lyon. ISBN: 978-2729707248.

Lou, T. & Karavasilis, T.L. 2018. Time-dependent assessment and deflection prediction of prestressed concrete beams with unbonded CFRP tendons. *Composite Structures*, 194, pp.365-376. Available at: https://doi.org/10.1016/j.compstruct.2018.04.013.

Mebsout, H., Krour, B. & Bachir Bouiadjra, M. 2018. Enhacing Pre-stressed Concrete Beam's Capacity Using Externally Bonded Pre-stressed Composite Plate. In: Abdelbaki, B., Safi, B. & Saidi, M. (Eds.) *Proceedings of the Third International Symposium on Materials and Sustainable Development. SMSD 2017*. Cham: Springer, pp.95-104. Available at: https://doi.org/10.1007/978-3-319-89707-3_12.

Mohamed, B.B., Abdelouahed, T., Samir, B. & El Abbas, A.B. 2009. Approximate analysis of adhesive stresses in the adhesive layer of plated RC beams. *Computational Materials Science*, 46(1), pp.15-20. Available at: https://doi.org/10.1016/j.commatsci.2009.01.020.

Mostakhdemin Hosseini, M.R., Dias, S.J.E. & Barros, J.A.O. 2016. Flexural strengthening of reinforced low strength concrete slabs using prestressed NSM CFRP laminates. *Composites Part B: Engineering*, 90, pp.14-29. Available at: https://doi.org/10.1016/j.compositesb.2015.11.028.

Páez, P.M. 2023. A simplified approach to determine the prestress loss and time-dependent deflection in cracked prestressed concrete members, prestressed with fiber reinforced polymers or steel tendons. *Engineering Structures*, 279, art.number:115523. Available at: https://doi.org/10.1016/j.engstruct.2022.115523.

Páez, P.M. & Sensale-Cozzano, B. 2021. Time-dependent analysis of simply supported and continuous unbonded prestressed concrete beams. *Engineering Structures*, 240, art.number:112376. Available at: https://doi.org/10.1016/j.engstruct.2021.112376.

Rezazadeh, M., Barros, J. & Costa, I. 2015. Analytical approach for the flexural analysis of RC beams strengthened with prestressed CFRP. *Composites Part B: Engineering*, 73, pp.16-34. Available at: https://doi.org/10.1016/j.compositesb.2014.12.016.

Smith, S.T. & Teng, J.G. 2001. Interfacial stresses in plated beams. *Engineering Structures*, 23(7), pp.857-871. Available at: https://doi.org/10.1016/s0141-0296(00)00090-0.

Tounsi, A. & Benyoucef, S. 2007. Interfacial stresses in externally FRP-plated concrete beams. *International Journal of Adhesion and Adhesives*, 27(3), pp.207-215. Available at: https://doi.org/10.1016/j.ijadhadh.2006.01.009.

Tounsi, A., Hassaine Daouadji, T., Benyoucef, S. & Adda bedia, E.A. 2009. Interfacial stresses in FRP-plated RC beams: Effect of adherend shear deformations. *International Journal of Adhesion and Adhesives*, 29(4), pp.343-351. Available at: https://doi.org/10.1016/j.ijadhadh.2008.06.008.

Zhang, H., Guo, Q.-Q. & Xu, L.-Y. 2023. Prediction of long-term prestress loss for prestressed concrete cylinder structures using machine learning. *Engineering Structures*, 279, art.number:115577. Available at: https://doi.org/10.1016/j.engstruct.2022.115577.

Investigación analítica del comportamiento interfacial de una viga de hormigón pretensada reforzada con una placa pretensada unida con FRP

Hanane Mebsout[a], *Mohamed Atif* Benatta[b],
Baghdad Krour[b], **autor de correspondencia**, *Oussama* Benachour[b],
Mohamed Bachir Bouiadjra[bc], *Nacer* Rahal[ad]

[a] Universidad Mustapha Stambouli,
Mascara, República Argelina Democrática y Popular

[b] Universidad de Djillali Liabes, Laboratorio de Estructuras y Materiales Avanzados en Ingeniería Civil y Obras Públicas (LSMAGCTP),
Sidi Bel Abbes, República Argelina Democrática y Popular

[c] Agencia Temática de Investigación en Ciencia y Tecnología,
Argel, República Argelina Democrática y Popular

[d] Universidad de Ciencias y Tecnología,
Laboratorio de Estructura Mecánica y Estabilidad de la Construcción,
Orán, República Argelina Democrática y Popular

CAMPO: ingeniería civil, materiales
TIPO DE ARTÍCULO: artículo científico original

Resumen:

Introducción/objetivo: El uso de materiales compuestos para reforzar estructuras de hormigón armado es una práctica muy común en la ingeniería civil. Sin embargo, la construcción con hormigón pretensado no suele utilizar este método. El objetivo principal del presente estudio es ampliar el uso de materiales compuestos para reforzar vigas de hormigón pretensado, considerando el efecto de la concentración de tensiones interfaciales en el comportamiento global de dichas estructuras.

Métodos: Se propone un nuevo modelo analítico que considera cómo los cambios en el pretensado de la viga de hormigón armado afectan las tensiones de interfaz. Se considera una función polinómica que expresa la variación de la forma geométrica del cable, así como las pérdidas instantáneas y no instantáneas de la viga de hormigón pretensado, para abordar el problema de la concentración de tensiones en la interfaz entre la placa adhesiva y el hormigón.

Resultados: Los principales hallazgos de la presente investigación demuestran que, en presencia del cable pretensado, las tensiones de interfaz disminuyen de manera no significativa; pero, a medida que aumenta la fuerza de pretensado aplicada a la placa de FRP, se observa un aumento más sustancial de las tensiones de interfaz.

Conclusión: Debido a un alto grado de tensiones de contacto en el extremo de la placa, el riesgo de desprendimiento es mayor y se recomienda un mecanismo de anclaje en el borde de la placa.

Palabras claves: viga de hormigón pretensado, compuestos FRP, tensiones interfaciales, orientación de fibras, refuerzo.

Аналитическое исследование межфазного взаимодействия предварительно напряженной бетонной балки, усиленной преднапряженной композитной арматурой

Анан Мебсоут[а], *Мухаммед Атиф* Бинатта[б],
Багдад Кроур[б], **корреспондент**, *Оссама* Беначур[б],
Мухамед Башир Буяжера[бв], *Насер* Рахал[аг]

[а] Университет им. Мустафы Стамбули,
г. Маскара, Алжирская Народная Демократическая Республика

[б] Университет Джиллали Лиабеса,
Лаборатория конструкций и передовых материалов в гражданском строительстве и общественных работах (LSMAGCTP),
г. Сиди-Бель-Аббес, Алжирская Народная Демократическая Республика

[в] Тематическое агентство научно-технических исследований,
г. Алжир, Алжирская Народная Демократическая Республика

[г] Университет естественных наук и технологий,
Лаборатория машиностроения и прочности конструкций,
г. Оран, Алжирская Народная Демократическая Республика

РУБРИКА ГРНТИ: 67.11.00 Строительные конструкции,
67.09.33 Бетоны. Железобетон. Строительные растворы, смеси, составы
ВИД СТАТЬИ: оригинальная научная статья

Резюме:

Введение/цель: Использование композитных материалов для усиления железобетонных конструкций в настоящее время является весьма распространенной практикой в области гражданского строительства. Однако в конструкциях из предварительно напряженного бетона этот метод обычно не используется. Главной целью данного исследования является расширение использования композитных материалов для усиления предварительно напряженных бетонных балок с учетом влияния концентрации межфазных напряжений на общее поведение таких конструкций.

Методы: В статье представлена новая аналитическая модель, учитывающая, как изменения предварительного напряжения преднапряженных железобетонных балок влияют на граничные напряжения. Для решения проблемы концентрации напряжений на месте соединения клей-плита-бетон рассматривается полиномиальная функция, выражающая изменение геометрической формы кабеля, а также временные и не постоянные деформации на предварительно напряженной бетонной балке.

Результаты: Основные результаты настоящего исследования показывают, что при предварительном напряжении кабеля граничные напряжения незначительно уменьшаются, однако по мере увеличения усилия предварительного напряжения, приложенного к термопластику FRP, наблюдается существенное увеличение граничных напряжений.

Вывод: Вследствие высокой степени контактных напряжений на грани плиты возрастает риск расслоения, поэтому рекомендуется использовать анкерный крепеж по ее краям.

Ключевые слова: предварительно напряженная бетонная балка, композиты FRP, межфазные напряжения, ориентация волокон, упрочнение.

Аналитичко испитивање понашања на интерфејсу код преднапрегнуте бетонске греде ојачане преднапрегнутом плочом везаном композитним материјалима

Анан Мебсоут[а], *Мухамед Атиф* Бината[б],
Багдад Кроур[б], **аутор за преписку**, *Осама* Беначур[б],
Мухамед Башир Бујажера[бв], *Насер* Рахал[аг]

[а] Универзитет „Мустафа Стамболи”, Маскара, Народна Демократска Република Алжир

[б] Универзитет „Ђилали Лиабес”, Лабораторија за напредне конструкције и материјале у грађевинарству и јавним радовима (LSMAGCTP), Сиди Бел Абес, Народна Демократска Република Алжир

[в] Тематска агенција за истраживање науке и технологије,
Алжир, Народна Демократска Република Алжир

[г] Универзитет природних наука и технологије,
Лабораторија за машинске структуре и стабилност конструкције,
Оран, Народна Демократска Република Алжир

ОБЛАСТ: грађевинарство, материјали
КАТЕГОРИЈА (ТИП) ЧЛАНКА: оригинални научни рад

Сажетак:

Увод/циљ: Употреба композитних материјала за армирање армиранобетонских конструкција данас је веома честа у области грађевинарства. Међутим, овај метод се обично не користи код преднапрегнутих бетонских конструкција. Основни циљ овог рада јесте да прошири употребу композитних материјала на армирање преднапрегнутих бетонских греда узимајући у обзир утицај концентрације напона на интерфејсу на укупно понашање ових конструкција.

Методе: Предлаже се нови аналитички модел који узима у обзир начин на који преднапрегнутост преднапрегнутих бетонских греда утиче на напоне на интерфејсу. Разматра се полиномска функција која изражава варијацију геометријског облика кабла, као и тренутне и нетренутне губитке преднапрегнуте бетонске греде ради решавања питања концентрације напона на интерфејсу везиво-плоча-бетон.

Резултати: Главни налази овог испитивања показују да се, у присуству преднапрегнутости кабла, напони на интерфејсу незнатно смањују. Међутим, са повећавањем силе преднапрезања примењене на ФРП плочу уочава се знатније повећање напона на интерфејсу.

Закључак: Услед високог степена контактних напона на крају плоче, ризик од одвајања постаје већи, па се препоручује механизам за анкерисање на ивици плоче.

Кључне речи: преднапрегнута бетонска греда, ФРП композити, напони на интерфејсу, оријентација влакана, ојачавање.

Paper received on: 18.10.2024.
Manuscript corrections submitted on: 26.03.2025.
Paper accepted for publishing on: 27.03.2025.